Rapid Communication

JCBFM

Journal of Cerebral Blood Flow & Metabolism
2018, Vol. 38(10) 1690–1700

DOI: 10.1177/0271678X18786359
journals.sagepub.com/home/jcbfm
SAGE

Evidence from functional ultrasound imaging of enhanced contralesional microvascular response to somatosensory stimulation in acute middle cerebral artery occlusion/reperfusion in rats: A marker of ultra-early network reorganization?

Clément Brunner[1,2], Marie Korostelev[1], Sushmitha Raja[1], Gabriel Montaldo[2], Alan Urban[2] and Jean-Claude Baron[1,3]

Abstract

Following middle cerebral artery (MCA) stroke, enhanced contralesional evoked responses have been consistently reported both in man and rodents as part of plastic processes thought to influence motor recovery. How early this marker of large-scale network reorganization develops has however been little addressed, yet has clinical relevance for rehabilitation strategies targeting plasticity. Previous work in mice has reported enhanced contralesional responses to unaffected-side forepaw stimulation as early as 45 min after MCA small branch occlusion. Using functional ultrasound imaging (fUSi) in anesthetized rats subjected to distal temporary MCA occlusion (MCAo), we assessed here (i) whether enhanced contralesional responses also occurred with unaffected-side whisker pad stimulation, and if so, how early after MCAo; and (ii) the time course of this abnormal response during occlusion and after reperfusion. We replicate in a more proximal MCA occlusion model the earlier findings of ultra-early enhanced contralesional evoked responses. In addition, we document this phenomenon within minutes after MCAo, and its persistence throughout the entire 90-min occlusion as well as 90-min reperfusion periods studied. These findings suggest that plastic processes may start within minutes following MCAo in rodents. If replicated in man, they might have implications regarding how early plasticity-enhancing therapies can be initiated after stroke.

Keywords

Evoked responses, functional ultrasound imaging, hemodynamic response, plasticity, sensory stimulation

Received 5 March 2018; Revised 17 May 2018; Accepted 7 June 2018

Introduction

Following stroke-induced focal brain damage, adaptive plastic reorganization at both the synaptic and large-scale cortical network levels results in gradual improvement of lost functions.[1,2] Functional imaging studies in the early post-stroke period in man have provided new insights into large-scale network reorganization, notably they consistently documented enhanced contralesional primary cortices activations, resulting in inter-hemispheric activation imbalance.[3–8] As applied to the primary sensorimotor cortex (SM1), this finding

[1]Inserm U894, Université Paris Descartes, Paris, France
[2]Neuro-Electronics Research Flanders (NERF; A Research Initiative by IMEC, VIB and KU Leuven), Catholic University Leuven, Leuven, Belgium
[3]Department of Neurology, Hôpital Sainte-Anne, Paris, France

The first two authors contributed equally to this work.
The last two authors share senior authorship.

Corresponding author:
Jean-Claude Baron, Department of Neurology, Hôpital Sainte-Anne, Inserm U894, Paris, France.
Email: jean-claude.baron@inserm.fr

has been replicated with both motor execution and passive arm movement – i.e. proprioceptive stimulation.[6] Importantly, although overall such imbalance tends to return towards physiological levels as recovery proceeds,[4,6,7] the higher the prevailing contralesional SM1 activation, the worse the performance – suggesting maladaptive plasticity.[9,10] These observations have led to novel therapeutic approaches to restore the interhemispheric balance, involving either stimulating ipsilesional SM1 or inhibiting contralesional SM1 by means of specific rehabilitation paradigms or non-invasive transcranial neuronal stimulation or inhibition, which effectively improve motor performance.[11–14] Mechanistically, contralesional SM1 over-activations are thought to reflect loss of inhibitory transcallosal projections from directly stroke-affected or disconnected ipsilesional M1.[15]

One critical but debated point, however, is how early therapies targeting plasticity should begin after stroke.[16] Given the significant practical and ethical issues involved in performing ultra-early investigations in stroke patients, very little information is available regarding network reorganization earlier than one week post-stroke.[17] Animal models are better suited to address this issue, particularly those implementing middle cerebral artery occlusion (MCAo), the commonest cause of ischemic stroke in man.

The few available animal functional MRI (fMRI) studies on post-stroke reorganization have shown patterns remarkably similar to those described above in man. Using somatosensory stimulation, they have consistently reported abnormally elevated contralesional SM1 activations,[18–22] that tend to normalize in parallel with behavioral recovery,[18–20] while their persistence predicts poor motor recovery.[19,21] Again, the putative mechanism for contralesional SM1 over-activations is the loss of inhibitory transcallosal input from the damaged SM1.[18] However, the earliest time-point contralesional SM1 activation which was assessed in these studies was 24 h.[19]

At variance from the above fMRI studies indirectly assessing neuronal response by means of the hemodynamic response, two additional studies directly assessed neuronal activity. Using cortical photothrombosis in mice – a model that does not mimic well human stroke – Takatsuru et al.[23] found higher contralesional SM1 field potentials evoked by affected forepaw stimulation at post-stroke days 2–3 (earliest timepoint assessed). Of greater relevance to the hyper-acute plasticity issue, using voltage-sensitive dyes (VSDs) in mice, Mohajerani et al.[24] found enhanced contralesional S1 response to unaffected forepaw stimulation, administered 45 min following partial S1 infarction induced by photothrombotic permanent small MCA branch occlusion. Earlier time-points were not assessed in this seminal study, while the stroke model used was representative of the clinical situation of distal field occlusions resulting from small emboli, but not of the more common situation – and more relevant to long-term rehabilitation – of acute proximal MCA occlusion. In addition, serial assessment of this abnormal response during occlusion, and the effects of reperfusion – which has become standard-of-care in clinical stroke[25] – were not part of the experimental protocol.

Our aim in the present study was to replicate the above finding of abnormally elevated contralesional response to unaffected-side stimulation, but with the following key differences: (i) assessing this response immediately following, and serially during, MCAo in order to determine its dynamics, rather than at a single 45-min time-point; (ii) using a temporary MCAo model mimicking the frequent clinical situation of proximal (distal stem) MCA occlusion with early recanalization; (iii) delivering stimulations serially after release of occlusion, to assess whether the abnormal response persists or quickly reverts after tissue reperfusion; and (iv) implementing whisker instead of forelimb stimulation, taking into consideration the location of the barrel field (S1BF) mostly within the cortical MCA territory, at variance from the forelimb cortical area which straddles its borders.[18,26,27] A final difference from Mohajerani et al. was that instead of directly assessing neuronal responses, we used functional ultrasound imaging (fUSi)[28–30] to assess hemodynamic responses, similar to clinically available fMRI. The newly developed fUSi technique (i) allows the microvasculature, specifically the cerebral blood volume (CBV), to be dynamically mapped across the cortical thickness,[31] as opposed to restricted to the cortical surface for VSDs;[24] and (ii) affords better spatial and temporal resolutions and greater sensitivity, and is less procedurally cumbersome, than fMRI.

Methods

Animals, anesthesia and craniotomy preparation

This investigation was performed in accordance with the National Institutes of Health Guide for Care and Use of Laboratory Animals. The protocol was approved by the Local Animal Ethics Committee of Paris 5 (CEEA 34) and conducted in accordance with Directive 2010/63/EU of the European Parliament.

Contralateral (i.e. contralesional) S1 responses to unaffected-side whisker stimulation during and after 90-min tMCAo were assessed using fUSi in 12 adult male Sprague-Dawley rats (250–350 g; Janvier Labs, France). Rats housed four per cage were kept in a 12-h reverse dark/light cycle environment at a temperature of 22°C with unlimited water and controlled

access to food (around 20 g per day per animal). For completeness, responses to affected-side whisker stimulation, interleaved with unaffected-side stimulation, will also be presented. Under spontaneous breathing of room air through a nose cone, the rat was anesthetized using isoflurane as follows: 5% for induction, 2.5–3% for skull surgery, then 1.5% for the MCAo procedure and throughout fUSi data acquisition. Throughout experiments, body temperature was controlled using a rectal probe and heating blanket, and SaO_2 was continuously monitored and remained within normal limits in all experiments. All subjects will be reported below. This manuscript was written up according to the ARRIVE guidelines for reporting animal experiments.

Skull surgery consisted first in skull thinning followed by two craniotomies to allow both fUSi data acquisition and distal MCAo.[31] Briefly, the rat head was fixed using a stereotaxic frame, the scalp was removed and the skull carefully cleaned. The skull was then gently thinned with a low-speed dental drill between bregma −2.0 and −4.0 mm, extending 6.5 mm bilaterally from the sagittal suture for fUSi acquisition. This coronal plane was selected based on the Paxinos and Watson stereotaxic atlas[32] in order to include S1BF, i.e. the stimulation target. The craniotomy then involved slowly and carefully peeling the skull without removing the dura. Throughout the procedure, cold Ringer-lactate solution was regularly applied over the surgical area to avoid overheating from drilling. The craniotomy was then protected by a layer of agarose until the imaging session started. Following a similar procedure, an additional 1 mm^2 craniotomy was performed over the left MCA (bregma +2.0 mm, lateral +7.0 mm). The animal was then moved and secured onto an air-suspended table to reduce mechanical noise, placing the head under the ultrasound probe. An acoustic gel was applied over the coronal craniotomy to ensure proper propagation of ultrasound. The ultrasonic transducer was then placed at 1.5 mm above this craniotomy (Figure 1(a)). The isoflurane level was then reduced and once the breathing pattern and rate were considered stable, the imaging session started (see imaging protocol below).

MCA occlusion

Distal left MCAo was carried out after the baseline fUSi acquisition session (see below), using Buchan's microclip method,[33] using a 1 mm surgical microclip (18055-04, Micro Serrefine, FST, USA) as detailed elsewhere[34] (see Figure 1(a)). This occlusion method was elected to allow effective transient occlusion and reperfusion. For this study, an occlusion duration of 90 min was chosen in order to ensure significant cortical ischemia, but also effective reperfusion.[35,36]

Stimulation paradigm

Two stimulation electrodes (Biopac Systems, Inc., USA) were inserted in each whisker pad prior to imaging (Figure 1(a)). The right and left whisker pads were alternatively stimulated by electrical pulses of 5 s duration, 0.7 mA intensity and 5 Hz frequency. For each whisker side, stimuli were spaced by 2-min rest periods. For each side, three stimulations were delivered near the end of the 30-min baseline fUSi acquisition period. Stimulations were then continuously delivered throughout the occlusion and reperfusion periods (see below). Whisker pad stimulations were time-locked with fUSi acquisition to allow subsequent analysis of hemodynamic responses within the fUSi time-series (see below).

fUSi data acquisition

A 30-min fUSi acquisition block was recorded in the baseline condition, which covered three stimulations per side delivered in the last 5 min of acquisition. fUSi acquisition was continued during the 90-min occlusion period and then again for 90 min after clip removal, but was interrupted twice for <5 min, first to allow MCA occlusion and second to allow clip removal (Figure 1(b)). Accurate head repositioning was ensured by a stereotaxic frame. fUS images were acquired at 1.43 Hz, i.e. one fUS image every 0.7 s. Acquired fUS images were processed in real-time on a dedicated GPU architecture[37] and stored in a solid-state drive (SSD) for subsequent off-line analysis.

fUSi data processing and analysis

In order to extract hemodynamic responses for each animal and each condition (i.e. baseline, occlusion and reperfusion), the rCBV data were analyzed as detailed elsewhere,[29] with minor modifications as follows: for each stimulation (left or right whisker pad) during baseline acquisition, each pixel of the coronal fUS image was normalized to that pixel's pre-stimulus average. To this end, blocks of 60 images (i.e. 42 s) were extracted in order to cover the 12 s before, 5 s during and 25 s after the end of each stimulation to allow the hemodynamic response to return to baseline. First, the three 42-s blocks for the three stimuli delivered during the baseline session were averaged. Any pixel was then considered as 'activated' if its signal exceeded the average plus 1.2 standard deviation of the 12-s pre-stimulation period. This allowed an 'activation map' to be generated (Figure 1(c)), which was subsequently smoothed by an 8×8 pixel Gaussian filter. Then, for each time-point over the 42-s hemodynamic response blocks, and separately for the baseline occlusion and reperfusion conditions, the mean rCBV across all

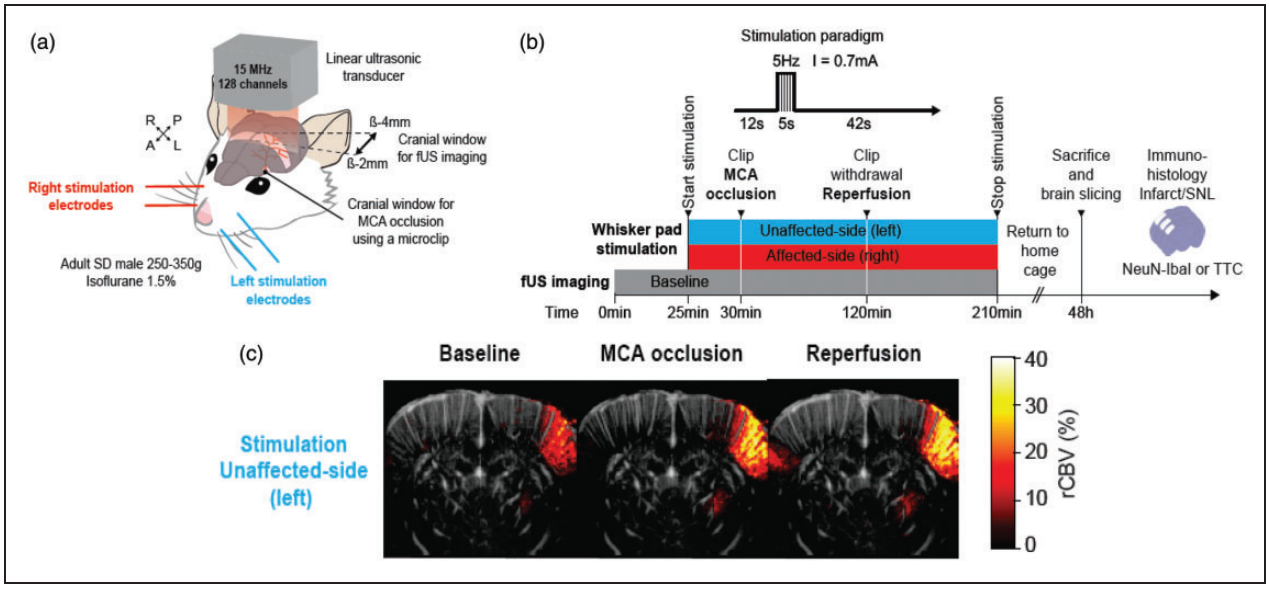

Figure 1. (a) 3D view of the rat head showing the coronal craniotomy (brown-shaded band) drilled between bregma −2.0 and −4.0 mm and extending 6.5 mm on each side from the sagittal suture for fUSi acquisition. The ultrasonic probe was positioned above the coronal craniotomy. This coronal plane was selected based on the Paxinos and Watson stereotaxic atlas[32] in order to include the S1 barrel field, i.e. the stimulation target. A smaller round-shaped 1 mm^2 craniotomy was performed at bregma +2.0 mm, lateral +7.0 mm to access the left MCA to place the microclip used for occlusion (black dot). Two pairs of stimulation electrodes (blue and red) were inserted in the whisker pads for stimulation of the unaffected and affected side, respectively. The stimulated area is shown in light gray shade. (b) Schematic representation of the experiment timelines. After baseline fUSi data acquisition (duration: 30 min which included the three runs of left and right whisker pad stimulation in the last 5 min), the left MCA was occluded (black arrowhead) for 90 min and the clip was then released (black arrowhead). Whisker pad stimulations (red and blue bars for left and right whisker pad stimulation, respectively) are depicted across the baseline, occlusion and reperfusion conditions. Each side was alternatively stimulated three times during the baseline period, and every 2 min throughout the occlusion and reperfusion periods. Interruptions in the stimulation bars represent the short time periods where the rat was removed from the experimental set-up to allow proceeding with MCAo and recanalization. Throughout the baseline, occlusion and reperfusion periods fUS images were acquired continuously every 0.7 s, except during the MCAo and reperfusion clip manipulations. After fUS imaging, rats were returned to their home cage for 48 h until perfusion-fixation for and immuno-histochemistry (see Methods) to assess infarction and selective neuronal loss (SNL); (c) Coronal fUSi image with superimposed "activated" pixels in response to whisker pad stimulation of the unaffected-side (left) whisker pad during baseline (image shown on the left), generated according to the voxel-based image processing procedures described in Methods. Activations are shown in % CBV increase compared to baseline (pseudo-colour scale on right of image). For illustration, similar images obtained during MCA occlusion and after reperfusion are also presented (middle and right, respectively), showing markedly increased contralesional rCBV responses to whisker stimulation in both conditions. Scale bar = 2.5 mm.

voxels present within these masks (expressed as percent of mean pre-stimulation rCBV) were plotted over time, creating fUSi 'time-series'. In order to assess the time course of the hemodynamic responses within the occlusion and reperfusion conditions, and specifically whether the enhanced contralesional response, if any, was already present early after MCAo, the time-series were averaged according to three successive 30-min blocks for occlusion, and similarly three 30-min blocks for reperfusion (see Figure 2).

fUSi data statistical analysis

A two-way repeated-measures (RMs) ANOVA assessing the main effects of time and condition was carried out on the averaged 42-s hemodynamic response time-series across all three conditions (namely, Baseline, Occlusion and Reperfusion). To this end, the 42-s blocks were averaged across the whole 90-min occlusion and reperfusion conditions. In case of statistically significant condition effect, post hoc Dunnett tests (i.e., implementing a correction for multiple tests) were then carried out assessing each 0.7-s time-point of the 42-s response for significant differences between baseline and the occlusion and reperfusion conditions separately.

rCBV

In order to determine the severity of MCAo-induced ischemia within the stimulated cortical area, as well as the degree of reperfusion achieved after recanalization,

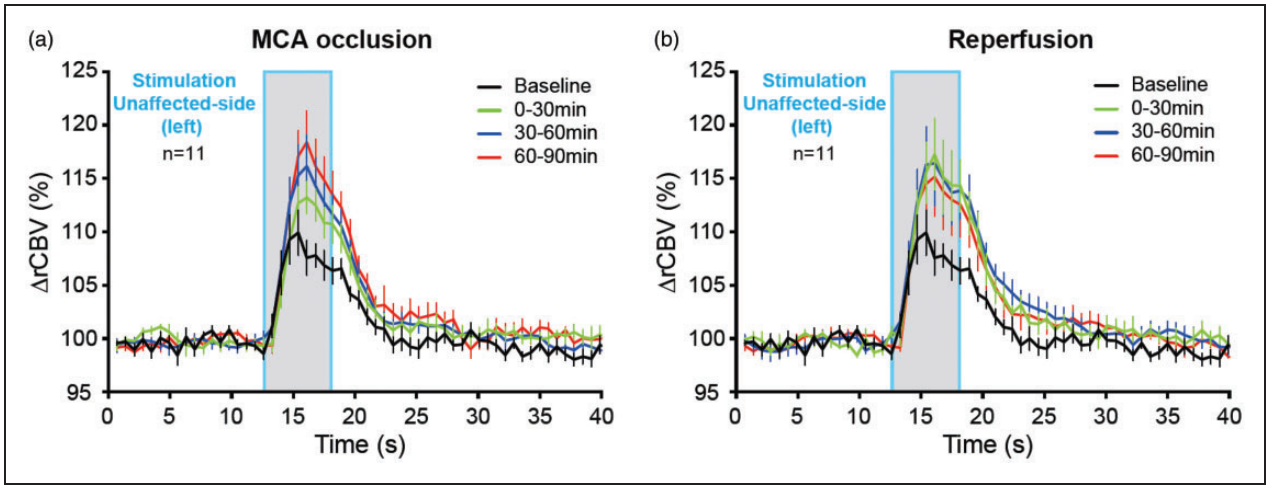

Figure 2. Time-course of hemodynamic responses in the S1BF area contralateral to left whisker pad stimulation (i.e. contralesional) before and during occlusion of the MCA (a), and following reperfusion (b). Mean (±SEM; $n = 11$ rats) %rCBV (i.e. percent change in rCBV relative to baseline) time-series for the contralesional hemisphere in response to unaffected-side (i.e. left) whiskers stimulation (grey bar; duration: 5 s) acquired at baseline (black) and for the three 30-min blocks acquired from 0 to 30 min (green), 30 to 60 min (blue) and 60 to 90 min (red) during occlusion (a) and similarly after recanalization (b). The data show the expected typical hemodynamic response at baseline, which is markedly enhanced during both occlusion and reperfusion; note an apparent decline in hemodynamic response across the three successive 30-min reperfusion blocks. See Methods for details, and Table 1 for statistical results.

which in turn should help to interpret the hemodynamic responses as determined above, we also determined resting-state rCBV within the same ROI as that used for the hemodynamic responses. To this end, the mean rCBV signal over 300 fUS images (i.e. 3.5 min) during non-stimulated periods was extracted at baseline (before stimulation), early after MCAo (as soon as the animal was repositioned under the ultrasonic probe), at 30 and 60 min after occlusion, immediately before reperfusion, and as soon as the animal was repositioned after reperfusion. For each animal, the rCBV values at each occlusion and reperfusion time-point were expressed as % of baseline.[38] A one-way RM-ANOVA was performed on the rCBV data ($n = 12$ rats) from the baseline, occlusion (four time-points) and reperfusion (one time-point) conditions, assessing the main effect of time.

Histopathology

Immediately after completion of fUSi data acquisition, agarose gel melted with ampicillin (100 µg/mL) was spread over the craniotomy, and the scalp was sutured. Intra-peritoneal buprenorphine (0.05 mg/mL) was then given to prevent post-surgery pain, and the animal was returned to its cage. After awakening, the animal was regularly assessed to detect any sign of pain. At the 48-h post-MCAo time-point, the animal was deeply anesthetized with sodium pentobarbital (100 mg/kg i.p.) and perfusion-fixation carried out as follows: the animal was transcardially perfused with 50 mL saline followed by 150 mL of 4% paraformaldehyde (PFA) in 0.1 M phosphate buffer saline (PBS; pH = 7.4), using a peristaltic pump and flow rate of 10 to 25 mL/min (Figure 1(b)). The brain was removed and placed overnight in 4% PFA fixative in PBS, and 40 µm thick sections across the MCA territory were prepared using a vibratome (Leica VT1000S, Leica Microsystems, Germany). For immunohistochemistry (IHC), six coronal slices (bregma +2.50, +1.00, −0.00, −1.00 −2.00 and −3.00 mm) were immunolabeled overnight with antibodies against the neuronal marker NeuN (1:1000; Millipore, USA) and the microglial activation marker Iba1 (1:500; Abcam, USA). The slices were then washed 3 × 10 min at room temperature followed by incubation with species-appropriate secondary antibodies conjugated to Alexa Fluor 488 nm (Molecular Probes, Life Technologies, France, 1:1000) in PBS, washed again (3 × 10 min) in PBS, and mounted with a DAPI Prolong Antifade kit (Molecular Probes, Life Technologies, France). Standardized images acquisition was performed with a digital slide scanner (Hamamatsu NanoZoomer, USA) at 20× magnification.

For unexpected technical reasons, perfusion-fixation was not feasible in four rats, in which the 2,3,5-triphenyltetrazolium chloride (TTC) staining method was carried out instead. At the 48-h post-MCAo time-point, the animal was deeply anesthetized with sodium pentobarbital (100 mg/kg i.p.) and the brain was carefully extracted and cut in 2-mm thick slices

Table 1. Results of the 2-way repeated-measures ANOVA of hemodynamic responses in the non-ischemic hemisphere to left-sided whisker pad stimulation at baseline, occlusion and reperfusion, and results of the post hoc Dunnett's tests (i.e. involving correction for multiple tests), comparing individual time-points for the occlusion and reperfusion conditions versus corresponding baseline time-points.

	Results
Baseline, occlusion and reperfusion	Condition effect: $p < 0.01$
Occlusion	TP comparison: condition to baseline TP 22–33: $p < 0.05$–0.0001
Reperfusion	TP comparison: condition to baseline TP 22–33: $p < 0.01$–0.0001

TP: time-point, i.e. each of the 0.7 s μDoppler image used for fUSi data analysis (to match Figure 2, TP 22 corresponds to 15.5 s, TP 33 to 23.1 s, etc.).

along the coronal plane. Brain slices were directly incubated into a 2%-TTC solution (in PBS) at 37°C for 15–20 min in the dark.[39,40] Active mitochondria in brain cells produce dehydrogenases that can enzymatically reduce TTC to formazan. Red staining is indicative of viable tissue, whereas local lack of staining at 48 h post MCAo is widely considered to represent infarcted tissue.[41,42]

Results

Hemodynamic responses

One rat was excluded from analysis of hemodynamic responses as no responses were detected at baseline, likely due to an unidentified technical/human failure; tMCAo nevertheless proceeded as per protocol. All remaining 11 rats survived throughout the entire protocol and are reported below.

Contralateral (contralesional) responses to unaffected-side (left) whiskers stimulation. In the baseline condition, clear-cut physiological responses were obtained in the hemisphere contralateral to the stimulated whisker pad, showing typical hemodynamic rCBV responses (Figure 2). Throughout both MCA occlusion and reperfusion, these responses were markedly greater than at baseline, as readily visible on mean time-series (Figure 2; findings also pictorially illustrated in Figure 1(c)). The two-way RM-ANOVAs showed a significant condition effect ($p < 0.01$), with post hoc tests documenting for both the occlusion and reperfusion conditions, the presence of significantly higher rCBV for numerous individual post-stimulation time-points relative to baseline (Table 1). The time-series tended to evolve towards more physiological responses across the three successive 30-min reperfusion blocks (Figure 2).

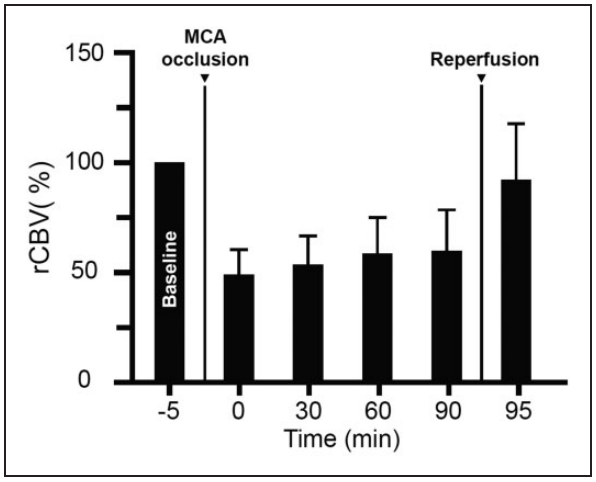

Figure 3. Resting-state rCBV time-course. rCBV (mean ± SD; $n = 12$; normalized to baseline = 100%) in the last 5 min of the baseline period (−5 min) and at 0, 30, 60 and 90 min after MCA occlusion, and almost immediately after recanalization (95 min), showing a clear-cut decline of rCBV throughout the occlusion period, followed by an immediate return to baseline rCBV after reperfusion. There was a highly significant ($p < 0.0001$) Time effect on repeated-measures ANOVA. See Results for detailed findings.

Affected-side (right) whiskers stimulation. During occlusion, contralateral (ipsilesional) hemodynamic responses to affected-side whiskers stimulation were, as expected, extremely weak, reflecting suppression of neuronal/hemodynamic response in the ischemic cortex, while clear responses resumed in the reperfusion phase (data not shown as outside the scope of this study). Ipsilateral (contralesional) responses were very weak and unstable, precluding any meaningful assessment of post-MCAo responses.

Resting-state rCBV time-course

Figure 3 shows the mean (±1 SD) normalized rCBV for the non-stimulated periods at baseline, during occlusion (four time-points: immediately after occlusion and after 30, 60 and 90 min), and immediately after reperfusion. Consistent with previous work[43–49] including our earlier study,[38] there was a clear-cut rCBV decline during MCAo, indicating effective ischemia, followed by immediate near-complete return of rCBV to pre-occlusion values after clip withdrawal, indicating effective capillary reperfusion. The RM-ANOVA revealed a significant time effect ($p < 0.0001$).

Histopathology

Brain sections were assessed blind to fUSi data. Immunofluorescence revealed definite ischemic lesions

in the left cortical MCA territory, consisting of isolated severe selective neuronal loss (SNL) with topographically congruent microglial activation in one rat, and frank infarction in three rats (associated with extensive peri-infarct SNL in one). No changes were detected in the remaining four rats. In rats for which TTC staining only was available, cortical stain loss was present in two rats and absent in two. Interestingly, there was a clear relationship between the presence of ischemic damage and normalized rCBV for each of the four time-points assessed during occlusion (all $p < 0.001$), with an apparent ~50% normalized rCBV threshold recorded immediately after MCAo discriminating damage versus no-damage outcome (see Supplemental Figure).

Discussion

This study documents significantly enhanced contralesional S1BF hemodynamic responses to unaffected-side whisker pad stimulation, suggesting neuron network reorganization occurring minutes after MCA occlusion in the rat. This enhanced response persisted not only throughout the 1.5-h MCA occlusion period but also during the entire 1.5-h reperfusion recording period, with an apparent trend towards more physiological response as time elapsed.

Our findings for the occlusion period are entirely consistent with Mohajerani et al.'s[24] observations, which derived from direct assessment of neuronal response using voltage sensitive dye imaging[24] (see Introduction). Although this supports the idea that the enhanced contralesional hemodynamic response found here reflects heightened evoked neuronal responses, further studies using fUSi coupled with VSDs or direct electrophysiological recording are needed to confirm this interpretation.

Our study has several novel features as compared to the above seminal study. First, our stroke model, namely distal MCAo followed by recanalization, mimics the now prevalent clinical situation of thrombectomy-treated large vessel occlusion.[25,50,51] Second, we elected to use whisker rather than forepaw stimulation because the S1BF area is located mainly within the cortical MCA territory, as compared to the forepaw area straddling its borders, such that the MCAo-induced cortical ischemia would be expected to cause transcallosal functional disruption of contralesional SIBF (see below). Third, we were able to assess evoked responses almost immediately following MCAo, which allowed documenting occurrence of contralesional upregulation within minutes of onset of MCAo, as compared to 45 min for Mohajerani et al. In turn, such an ultra-early adaptation would support these authors' contention that it reflects altered neurotransmission rather than neuronal rewiring. Fourth, contralesional responses were serially recorded during MCAo, showing persistence of the enhanced contralesional responses throughout the 1.5-h occlusion period, as compared to Mohajerani et al. who assessed the 45-min time-point only. Fifth, we assessed these responses not only during occlusion but also following reperfusion, as compared to during occlusion only in Mohajerani et al., showing persistence of the upregulated response throughout the 1.5-h reperfusion period. It will be important in further studies to investigate the time-course of this phenomenon both during extended and even permanent MCAo, as well as over extended reperfusion periods.

A few additional studies have used fMRI to map functional responses to somatosensory stimulation after experimental ischemic stroke, using as hemodynamic signal either BOLD[21,22,52] or ultra-small iron particles.[18–20] These techniques, and particularly the latter which also maps CBV, are similar to fUSi in as much as they also take advantage of neurovascular coupling to ascertain hemodynamic responses, therefrom neuronal responses are inferred. These studies consistently reported absent or very weak early ipsilesional SM1 responses to contralateral forepaw stimulation,[18–22,52] which subsequently tended to return peri-lesionally, except when motor deficits failed to recover.[18–22,52] More relevant to our study, they also consistently reported abnormally high contralesional SM1 activations,[18–22] which subsequently normalized in parallel with behavioral recovery and return of ipsilesional SM1 activation,[18–20] although their occasional persistence into the chronic stage was associated with poor recovery.[19,21] These findings bear striking similarity to findings in stroke patients (see Introduction). However, unlike our study, the earliest time-point of contralesional evoked response assessment in the above studies was 24 h.[19] By documenting that abnormal contralesional SM1 responses develop hyper-acutely, our study takes these previous observations back 24 h.

Of the above studies, one only implemented brief temporary MCAo.[52] These authors report reduced ipsilesional SM1 responses up to 24 h following 20-min MCAo, but no changes in contralesional responses. However, the very short ischemic period used resulted in only moderate hypoperfusion in SM1, and in turn pure SNL on post-mortem; in addition, fMRI was carried out after reperfusion, but not during the occlusion phase, limiting interpretation and comparison to our study.

The most widely accepted mechanism for enhanced contralesional responses is reduced transcallosal inhibition originating from the acutely ischemic cortex. In support of this hypothesis, similar to Mohajerani et al.'s observations regarding the forelimb cortex,[24] the enhanced contralesional response in our study was

associated with markedly reduced ipsilesional S1BF evoked responses, consistent with ischemia-induced neuronal shut-down. However, inconsistent with the transcallosal hypothesis, Mohajerani et al.[24] were unable to reproduce the enhanced contralesional responses by pharmacological inhibition of contralesional cortex, while they were unchanged in acallosal mice. Furthermore, that ipsilesional thalamic inactivation prevented them suggested a role for the thalamus.[24] To our knowledge, one published study only has assessed neuronal responses to unaffected-hand stimulation in man.[53] Using fMRI, these authors report the presence of both ipsilesional and contralesional activation during unaffected upper limb movement in chronic hemiplegic subjects, and although formal comparisons are not reported, no clear difference in contralesional response intensity relative to controls emerges from their Table 2 and Figure 2.[53] Unfortunately, the authors did not comment on this observation. Further work is required in both rodents and humans to clarify the mechanisms underlying this intriguing phenomenon. One potential approach in rodents would involve correlating fUSi responses with detailed assessment of white matter tracts connecting the ischemic hemisphere to contralesional SM1. This could be achieved by means of MR-based diffusion tensor imaging (DTI) both during occlusion and after reperfusion, together with fine histopathological mapping of damaged and preserved tracts.

As anesthetic agent, we used isoflurane, which is widely used in spontaneously breathing rodents because it permits to control the depth of anesthesia and to keep up physiological variables such as respiration.[54] Although isoflurane is known to affect cerebrovascular responses to blood pressure changes,[55,56] functional hemodynamic responses to sensory stimulation, including whisker stimulation, show no unusual features during isoflurane anesthesia,[52,55,57] as also reported using fUSi.[28,29,31,58] Even though isoflurane anesthesia may alter in unknown ways the hemodynamic response, it is highly unlikely the heightened contralesional hemisphere responses observed here reflect an isoflurane-related artefact because (i) pre-occlusion whisker stimulations were delivered after ~25 min of continuous isoflurane, ensuring steady-state (see Methods); (ii) a few minutes only separated the pre- to the early post-MCAo recordings (Figure 1(b)), and significantly enhanced responses were already observed in the first 10-min stimulation block, with no subsequent change (Figure 2); (iii) the shape, amplitude and time-course of recorded hemodynamic responses all appeared physiological (Figure 2); and (iv) our findings closely match those previously obtained using direct neuronal responses,[24] and can be explained by loss of transcallosal inhibitory input from the severely ischemic S1-BF cortex. Although fUSi is feasible in awake rodents in physiological conditions,[31,58] replicating the present MCAo study in awake animals would raise major logistical and ethical issues, including craniotomy-related pain and MCA clip placement and subsequent removal, interspersed with sensory stimulations.

This study was not designed to investigate the relationships between contralesional hemodynamic responses and histopathological outcome. Indeed, the former was to be assessed during a 90-min MCA occlusion and subsequent 90-min reperfusion epochs, i.e. when tissue damage is not yet fully determined given the add-on detrimental events that may develop following reperfusion.[59] Nevertheless, we elected to provide information on the range of histopathological changes present alongside the acute functional changes observed as being relevant. To this end, we collected the brains at 48 h post-reperfusion, a time when ischemic changes are largely stabilized, and determined tissue outcome using formal immunohistochemistry. Unfortunately, in four rats, unexpected technical problems led us to use TTC only, which is far from being as accurate, especially but not only with respect to SNL. Immunofluorescence revealed frank infarction in three rats, isolated SNL in one rat, and no changes in four rats, while TTC staining was absent in two rats. These findings overall suggested the presence of infarction in five rats and SNL in at least one rat, i.e. definite ischemic damage overall affecting ~50% of the subjects. Such variability in tissue outcome following short MCAo in Sprague-Dawley rats is consistent with the literature,[35] especially when as here MCA occlusion is not associated with ipsilateral common carotid artery occlusion.[60,61]

In conclusion, our study mimicking the clinically relevant situation of proximal MCAo with early recanalization has provided indirect evidence towards ultra-early – i.e. occurring within minutes – functional brain reorganization in the form of enhanced contralesional hemodynamic responses. Although enhanced neuronal responses would be expected to trigger plastic processes, that these findings truly reflect enhanced neuronal responses will need to be confirmed using direct cell recordings. Future studies will also need to decipher the underlying mechanisms in terms of disrupted neuronal ensembles/networks. Assuming our interpretations is supported by such studies, one potential implication would be that in man post-stroke plastic processes might start within minutes after symptom onset, which could in turn be targeted by ultra-early specific therapies.

Funding

The author(s) disclosed receipt of the following financial support for the research, authorship, and/or publication of this article: This work was supported by Inserm U894 and Paris

Descartes University, Paris; SANOFI, France (PhD scholarship for CB); SFNV, France (MSc scholarship for MK); ANR, France (salary for SR), Leducq foundation, grant 15CVD02 (support to CB, GM and AU). The authors are grateful to Jacques Epelbaum and Cécile Viollet for their support.

Declaration of conflicting interests

The author(s) declared the following potential conflicts of interest with respect to the research, authorship, and/or publication of this article: Alan URBAN is an independent consultant in brain imaging technologies

Authors' contributions

CB: concept and design, data acquisition, data analysis, manuscript revision.
MK: concept and design, data acquisition, manuscript revision.
SJ: data analysis, manuscript revision.
GM: data acquisition, data analysis, manuscript revision.
AU: concept and design, manuscript revision.
JCB: concept and design, data analysis, manuscript drafting, finalized manuscript for submission, revisions.

Supplementary material

Supplementary material for this paper can be found at the journal website: http://journals.sagepub.com/home/jcb

ORCID iD

Clément Brunner http://orcid.org/0000-0002-2567-4832

References

1. Cramer SC and Riley JD. Neuroplasticity and brain repair after stroke. *Curr Opin Neurol* 2008; 21: 76–82.
2. Nudo RJ. Recovery after damage to motor cortical areas. *Curr Opin Neurobiol* 1999; 9: 740–747.
3. Calautti C and Baron JC. Functional neuroimaging studies of motor recovery after stroke in adults: a review. *Stroke* 2003; 34: 1553–1566.
4. Calautti C, Leroy F, Guincestre JY, et al. Dynamics of motor network overactivation after striatocapsular stroke: a longitudinal PET study using a fixed-performance paradigm. *Stroke* 2001; 32: 2534–2542.
5. Cramer SC, Nelles G, Benson RR, et al. A functional MRI study of subjects recovered from hemiparetic stroke. *Stroke* 1997; 28: 2518–2527.
6. Favre I, Zeffiro TA, Detante O, et al. Upper limb recovery after stroke is associated with ipsilesional primary motor cortical activity: a meta-analysis. *Stroke* 2014; 45: 1077–1083.
7. Jaillard A, Martin CD, Garambois K, et al. Vicarious function within the human primary motor cortex? A longitudinal fMRI stroke study. *Brain* 2005; 128: 1122–1138.
8. Tang Q, Li G, Liu T, et al. Modulation of interhemispheric activation balance in motor-related areas of stroke patients with motor recovery: systematic review and meta-analysis of fMRI studies. *Neurosci Biobehav Rev* 2015; 57: 392–400.
9. Calautti C, Jones PS, Naccarato M, et al. The relationship between motor deficit and primary motor cortex hemispheric activation balance after stroke: longitudinal fMRI study. *J Neurol Neurosurg Psychiatry* 2010; 81: 788–792.
10. Calautti C, Naccarato M, Jones PS, et al. The relationship between motor deficit and hemisphere activation balance after stroke: a 3T fMRI study. *Neuroimage* 2007; 34: 322–331.
11. Carey JR, Kimberley TJ, Lewis SM, et al. Analysis of fMRI and finger tracking training in subjects with chronic stroke. *Brain* 2002; 125: 773–788.
12. Takahashi CD, Der-Yeghiaian L, Le V, et al. Robot-based hand motor therapy after stroke. *Brain* 2008; 131: 425–437.
13. Stagg CJ, Bachtiar V, O'Shea J, et al. Cortical activation changes underlying stimulation-induced behavioural gains in chronic stroke. *Brain* 2012; 135: 276–284.
14. Lindenberg R, Renga V, Zhu LL, et al. Bihemispheric brain stimulation facilitates motor recovery in chronic stroke patients. *Neurology* 2010; 75: 2176–2184.
15. Rossini PM, Calautti C, Pauri F, et al. Post-stroke plastic reorganisation in the adult brain. *Lancet Neurol* 2003; 2: 493–502.
16. Bernhardt J, Indredavik B and Langhorne P. When should rehabilitation begin after stroke? *Int J Stroke* 2013; 8: 5–7.
17. Volz LJ, Rehme AK, Michely J, et al. Shaping early reorganization of neural networks promotes motor function after stroke. *Cerebral Cortex* 2016; 26: 2882–2894.
18. Dijkhuizen RM, Ren J, Mandeville JB, et al. Functional magnetic resonance imaging of reorganization in rat brain after stroke. *Proc Natl Acad Sci U S A* 2001; 98: 12766–12771.
19. Dijkhuizen RM, Singhal AB, Mandeville JB, et al. Correlation between brain reorganization, ischemic damage, and neurologic status after transient focal cerebral ischemia in rats: a functional magnetic resonance imaging study. *J Neurosci* 2003; 23: 510–517.
20. Abo M, Chen Z, Lai LJ, Reese T, et al. Functional recovery after brain lesion – contralateral neuromodulation: an fMRI study. *Neuroreport* 2001; 12: 1543–1547.
21. Markus TM, Tsai SY, Bollnow MR, et al. Recovery and brain reorganization after stroke in adult and aged rats. *Ann Neurol* 2005; 58: 950–953.
22. Weber R, Ramos-Cabrer P, Justicia C, et al. Early prediction of functional recovery after experimental stroke: functional magnetic resonance imaging, electrophysiology, and behavioral testing in rats. *J Neurosci* 2008; 28: 1022–1029.
23. Takatsuru Y, Fukumoto D, Yoshitomo M, et al. Neuronal circuit remodeling in the contralateral cortical hemisphere during functional recovery from cerebral infarction. *J Neurosci* 2009; 29: 10081–10086.
24. Mohajerani MH, Aminoltejari K and Murphy TH. Targeted mini-strokes produce changes in interhemispheric sensory signal processing that are indicative of disinhibition within minutes. *Proc Natl Acad Sci U S A* 2011; 108: E183–E191.

25. Goyal M, Menon BK, van Zwam WH, et al. Endovascular thrombectomy after large-vessel ischaemic stroke: a meta-analysis of individual patient data from five randomised trials. *Lancet* 2016; 387: 1723–1731.
26. Hughes JL, Beech JS, Jones PS, et al. Mapping selective neuronal loss and microglial activation in the salvaged neocortical penumbra in the rat. *Neuroimage* 2010; 49: 19–31.
27. von Bornstadt D, Houben T, Seidel JL, et al. Supply-demand mismatch transients in susceptible peri-infarct hot zones explain the origins of spreading injury depolarizations. *Neuron* 2015; 85: 1117–1131.
28. Mace E, Montaldo G, Cohen I, et al. Functional ultrasound imaging of the brain. *Nat Methods* 2011; 8: 662–664.
29. Urban A, Mace E, Brunner C, et al. Chronic assessment of cerebral hemodynamics during rat forepaw electrical stimulation using functional ultrasound imaging. *Neuroimage* 2014; 101: 138–149.
30. Gesnik M, Blaize K, Deffieux T, et al. 3D functional ultrasound imaging of the cerebral visual system in rodents. *Neuroimage* 2017; 149: 267–274.
31. Urban A, Dussaux C, Martel G, et al. Real-time imaging of brain activity in freely moving rats using functional ultrasound. *Nat Methods* 2015; 12: 873–878.
32. Paxinos G, Watson C, Pennisi M, et al. Bregma, lambda and the interaural midpoint in stereotaxic surgery with rats of different sex, strain and weight. *J Neurosci Methods* 1985; 13: 139–143.
33. Buchan AM, Xue D and Slivka A. A new model of temporary focal neocortical ischemia in the rat. *Stroke* 1992; 23: 273–279.
34. Ejaz S, Williamson DJ, Ahmed T, et al. Characterizing infarction and selective neuronal loss following temporary focal cerebral ischemia in the rat: a multi-modality imaging study. *Neurobiol Dis* 2013; 51: 120–132.
35. Baron JC, Yamauchi H, Fujioka M, et al. Selective neuronal loss in ischemic stroke and cerebrovascular disease. *J Cereb Blood Flow Metab* 2014; 34: 2–18.
36. Macrae IM. Preclinical stroke research – advantages and disadvantages of the most common rodent models of focal ischaemia. *Br J Pharmacol* 2011; 164: 1062–1078.
37. Urban A, Golgher L, Brunner C, et al. Understanding the neurovascular unit at multiple scales: advantages and limitations of multi-photon and functional ultrasound imaging. *Adv Drug Deliv Rev* 2017; 119: 73–100.
38. Brunner C, Isabel C, Martin A, et al. Mapping the dynamics of brain perfusion using functional ultrasound in a rat model of transient middle cerebral artery occlusion. *J Cereb Blood Flow Metab* 2017; 37: 263–276.
39. Bederson JB, Pitts LH, Germano SM, et al. Evaluation of 2,3,5-triphenyltetrazolium chloride as a stain for detection and quantification of experimental cerebral infarction in rats. *Stroke* 1986; 17: 1304–1308.
40. Lay CC, Davis MF, Chen-Bee CH, et al. Mild sensory stimulation completely protects the adult rodent cortex from ischemic stroke. *PLoS One* 2010; 5: e11270.
41. Goldlust EJ, Paczynski RP, He YY, et al. Automated measurement of infarct size with scanned images of triphenyltetrazolium chloride-stained rat brains. *Stroke* 1996; 27: 1657–1662.
42. Lavie G, Teichner A, Shohami E, et al. Long term cerebroprotective effects of dexanabinol in a model of focal cerebral ischemia. *Brain Res* 2001; 901: 195–201.
43. Heiss WD, Graf R, Wienhard K, et al. Dynamic penumbra demonstrated by sequential multitracer PET after middle cerebral artery occlusion in cats. *J Cereb Blood Flow Metab* 1994; 14: 892–902.
44. McLeod DD, Parsons MW, Hood R, et al. Perfusion computed tomography thresholds defining ischemic penumbra and infarct core: studies in a rat stroke model. *Int J Stroke* 2015; 10: 553–559.
45. Pappata S, Fiorelli M, Rommel T, et al. PET study of changes in local brain hemodynamics and oxygen metabolism after unilateral middle cerebral artery occlusion in baboons. *J Cereb Blood Flow Metab* 1993; 13: 416–424.
46. Quast MJ, Wei J, Huang NC, et al. Perfusion deficit parallels exacerbation of cerebral ischemia/reperfusion injury in hyperglycemic rats. *J Cereb Blood Flow Metab* 1997; 17: 553–559.
47. Sakoh M, Rohl L, Gyldensted C, et al. Cerebral blood flow and blood volume measured by magnetic resonance imaging bolus tracking after acute stroke in pigs: comparison with [(15)O]H(2)O positron emission tomography. *Stroke* 2000; 31: 1958–1964.
48. Young AR, Sette G, Touzani O, et al. Relationships between high oxygen extraction fraction in the acute stage and final infarction in reversible middle cerebral artery occlusion: an investigation in anesthetized baboons with positron emission tomography. *J Cereb Blood Flow Metab* 1996; 16: 1176–1188.
49. Zaharchuk G, Yamada M, Sasamata M, et al. Is all perfusion-weighted magnetic resonance imaging for stroke equal? The temporal evolution of multiple hemodynamic parameters after focal ischemia in rats correlated with evidence of infarction. *J Cereb Blood Flow Metab* 2000; 20: 1341–1351.
50. Albers GW. Thrombectomy for stroke at 6 to 16 hours with selection by perfusion imaging. *N Engl J Med* 2018; 378: 708–718.
51. Nogueira RG, Jadhav AP, Haussen DC, et al. Thrombectomy 6 to 24 hours after stroke with a mismatch between deficit and infarct. *N Engl J Med* 2018; 378: 11–21.
52. Sicard KM, Henninger N, Fisher M, et al. Long-term changes of functional MRI-based brain function, behavioral status, and histopathology after transient focal cerebral ischemia in rats. *Stroke* 2006; 37: 2593–2600.
53. Cramer SC, Mark A, Barquist K, et al. Motor cortex activation is preserved in patients with chronic hemiplegic stroke. *Ann Neurol* 2002; 52: 607–616.
54. Alstrup AK and Smith DF. Anaesthesia for positron emission tomography scanning of animal brains. *Lab Anim* 2013; 47: 12–18.
55. Ayata C, Dunn AK, Gursoy OY, et al. Laser speckle flowmetry for the study of cerebrovascular physiology in normal and ischemic mouse cortex. *J Cereb Blood Flow Metab* 2004; 24: 744–755.

56. Wang Z, Schuler B, Vogel O, et al. What is the optimal anesthetic protocol for measurements of cerebral autoregulation in spontaneously breathing mice? *Exp Brain Res* 2010; 207: 249–258.
57. Joutel A, Monet-Lepretre M, Gosele C, et al. Cerebrovascular dysfunction and microcirculation rarefaction precede white matter lesions in a mouse genetic model of cerebral ischemic small vessel disease. *J Clin Invest* 2010; 120: 433–445.
58. Tiran E, Ferrier J, Deffieux T, et al. Transcranial functional ultrasound imaging in freely moving awake mice and anesthetized young rats without contrast agent. *Ultrasound Med Biol* 2017; 43: 1679–1689.
59. Bai J and Lyden PD. Revisiting cerebral postischemic reperfusion injury: new insights in understanding reperfusion failure, hemorrhage, and edema. *Int J Stroke* 2015; 10: 143–152.
60. Brint S, Jacewicz M, Kiessling M, et al. Focal brain ischemia in the rat: methods for reproducible neocortical infarction using tandem occlusion of the distal middle cerebral and ipsilateral common carotid arteries. *J Cereb Blood Flow Metab* 1988; 8: 474–485.
61. Chen ST, Hsu CY, Hogan EL, et al. A model of focal ischemic stroke in the rat: reproducible extensive cortical infarction. *Stroke* 1986; 17: 738–743.